ELSEVIER

Experimental Thermal and Fluid Science 22 (2000) 35–44

Experimental Thermal and Fluid Science

www.elsevier.nl/locate/etfs

Analysis of pool boiling within smooth and grooved tubes

J.C. Passos *, R.F. Reinaldo

Universidade Federal de Santa Catarina, Departamento de Engenharia Mecânica, LABSOLAR-NCTS, 88010-970 Florianópolis-SC, Brazil

Received 14 July 1999; received in revised form 19 February 2000; accepted 6 March 2000

Abstract

This work presents experimental data for R-113 pool boiling, at atmospheric pressure and moderate heat flux, inside vertical and horizontal aluminum open-ended tubes, whose internal surfaces are either smooth or grooved. The tube length is 40 mm and the internal diameters of the smooth and the grooved tubes are 16.64 and 15.88 mm, respectively. The results are presented and discussed in relation to the heat transfer coefficients and compared with the Cooper and the Forster and Zuber empirical correlations. For all the tests, the heat transfer coefficient of the grooved tube is higher than that of the smooth tube. For horizontal tubes, an elongated bubble at the top region promotes a better local heat transfer coefficient as is indicated by the lower temperature than that of the bottom region, where the bubbles are isolated.

Keywords: Enhanced boiling; Nucleate boiling; Grooved surface; Nucleation

1. Introduction

Pool boiling heat transfer can be an efficient mode of wall cooling. Several studies [1,2] have considered the enhancement of the heat transfer coefficient during the nucleate boiling regime, and the study of Fujii et al. [3] has presented experimental results for boiling on wall surfaces of horizontal tubes with millimetric grooves. The interest of these studies applies to many two-phase flow applications such as solar energy thermosyphons or evaporators. For thermal control in satellite applications, the processes of liquid to vapor phase-change, in heat pipes and capillary pump devices, should be without bubbles. However, for design and selection of devices for space applications, knowledge of the onset of nucleate boiling is important [4,5]. Bergles [6] presented a review outlining the exponential increase of the number of papers, reports and patents, on enhanced heat transfer and estimated the number to be over 500. Bergles [6] named those trends as a second-generation heat transfer technology and found four areas of interest: structured surfaces for shellside boiling, rough surfaces in tubes, offset strip fins, and microfin tubes for refrigerant evaporators and condensers. In the 1990s, specialized textbooks were published; Thome's [7] and Webb's [8], for instance, confirmed Bergles's forecast.

In the sequence of this introduction we will present a brief review of the different mechanisms of the nucleate boiling regime, followed by a presentation of empirical correlations which will be tested in this work.

The objective of this work is to investigate the heat transfer mechanisms of R-113 pool boiling, at atmospheric pressure and moderate heat flux, inside horizontal and vertical open-ended tubes whose internal surfaces are either smooth or grooved. The resulting experimental data are compared with the Cooper and the Forster–Zuber empirical correlations.

1.1. Nucleate boiling mechanisms

In order to explain some phenomena tied to the enhancing boiling problem, it is interesting to note the main results obtained by Ishibashi and Nishikawa [9]. They studied the pool boiling problem in the annular space between a vertical copper cylindrical heater and various glass tubes with different internal diameters. Eight boiling spaces with dimensions ranging from 1 to 20 mm were tested. Ishibashi and Nishikawa [9] presented two regimes for nucleate boiling in narrow spaces, the first one characterized by isolated bubbles and the second by coalesced bubbles. In the second regime, bubbles can become squeezed, causing, at moderate heat flux, an increase in the heat transfer

* Corresponding author. Tel.: +55-48-3319379; fax: +55-48-2341519.

E-mail address: jpassos@emc.ufsc.br (J.C. Passos).

0894-1777/00/$ - see front matter
PII: S0894-1777(00)00008-X

Nomenclature

b	opening of the groove, μm
c_p	specific heat, kJ/(kg K)
h	heat transfer coefficient, W/(m^2 K)
h_{lv}	latent heat vaporization, kJ/kg
k	liquid conductivity, W/(m K)
M	molecular weight, kg/kmol
p	pressure, Pa
p_r	reduced pressure, dimensionless
q	heat flux, W/m^2 or kW/m^2
Rp	rugosity, μm
s	boiling space dimension, m
t	depth of the groove, μm
T	temperature, °C
v	specific volume, m^3/kg

Greek symbols

ΔT	wall superheat, $\Delta T = T_w - T_{sat}$, K
μ	viscosity, Pa s
ρ	density, kg/m^3
σ	surface tension, N/m

Subscripts

c	critical
exp	experimental
FZ	Forster–Zuber
i	inside
l	liquid
sat	saturation
v	vapor
w	wall

coefficient. This phenomenon has been attributed to the vaporization of a liquid film between the squeezed or coalesced bubble and the heater.

For nucleate boiling of saturated water in an isolated bubble regime, Ishibashi and Nishikawa [9] found the following relation between the heat transfer coefficient (h) and the heat flux (q):

$$h \propto q^n, \tag{1}$$

where n is equal to 2/3. General range value of n is between 0.6 and 0.8 as reported by Stephan [10]. At a constant heat flux, h increases, as the characteristic length (s) of the narrow space is reduced according to $h \propto q^{2/3}s^{-0.13}$. At atmospheric pressure, $s = 5.04$ mm and $\Delta T = 6.7$ K, the value of h is of the order of 7000 W/(m^2 K) and the corresponding photographs of this isolated bubble region show the spaced bubbles on the heater.

From the data of Ishibashi and Nishikawa [9], for ethyl alcohol, at atmospheric pressure and for heat flux between 9.1 and 9.9 kW/m^2, the heat transfer coefficient for an isolated bubble regime, when $s = 2.36$ mm, is 1653 W/(m^2 K). Without confinement, with $s = 82.5$ mm, this coefficient is 1000 W/(m^2 K) and for a coalesced bubble process, for $s = 0.97$ mm, it is 3846 W/m^2 K. These results show the existence of two heat transfer mechanisms. Under the isolated bubble mechanism, the augmentation of the heat transfer coefficient, when $s = 2.36$ mm, can be explained by the increase of the number of the nucleation sites. The significant augmentation of the heat transfer coefficient, when $s = 0.97$ mm, is caused by the presence of squeezed, or coalesced, bubbles on the heated surface. Even these two different heat transfer mechanisms are obtained, in [9], by variation of s, we can expect similar effects on the heat transfer coefficient if the same vapor configurations are present.

Nishikawa and Fujita [1] reported their own experimental and theoretical results and those of other researchers regarding the effect of surface orientation in unconfined saturated water pool boiling on a flat copper plate. With moderate values of heat flux (<170 kW/m^2), two different mechanisms in nucleate boiling were observed, depending on the tilt angle. When the boiling surface is facing downwards, the boiling mechanism changes from an isolated bubbles regime to an elongated or coalesced bubbles regime, while the tilt angle increases from 0° to 175°. As the work of Ishibashi and Nishikawa [9] shows, boiling with elongated bubble regime promotes the vaporization of the liquid film between the bubble and the wall, allowing a higher heat transfer coefficient than in the case of the isolated bubble regime. When the heat flux is high (>170 kW/m^2) the heat transfer coefficient is independent of the tilt angle. This behavior shows that the nucleate boiling mechanism at high heat flux is apparently influenced more by the characteristics of the surface conditions than by the presence of large bubbles on the heated plate.

Nishikawa and Fujita [1] showed the effect of surface roughness on heat transfer as a function of the tilt angle and the heat flux. For vertical plates the rough surface gives a higher heat transfer coefficient than the smooth surface. This trend is confirmed by the previous works on boiling, as presented in Chapter 16 of [10], and it is due to the higher nucleation site density in a rough surface when compared to a smooth surface, at a given wall superheat, [11]. At a tilt angle higher than 150° and for low heat flux (<100 kW/m^2) there is no influence of the surface roughness; this effect suggests a better boiling heat transfer only when the heat flux is high.

1.2. Empirical correlations

Among the great number of empirical correlations for nucleate boiling we have chosen those of Forster and Zuber (see [11,12]). These correlations were obtained from experimental data on developed or intensive nucleate boiling regime.

The Forster and Zuber correlation is based on dimensionless parameters, the Reynolds and the Prandtl

numbers of the bubble, and according to a power law, [10,11]. It is given as

$$h_{FZ} = 0.0012\left(\frac{k_l^{0.79}\, c_{pl}^{0.45}\, \rho_l^{0.49}}{\sigma^{0.5}\, \mu_l^{0.29} h_{lv}^{0.24} \rho_v^{0.24}}\right) \times \left[T_w - T_{sat}(p_l)\right]^{0.24} \left[p_{sat}(T_w) - p_{atm}\right]^{0.75}, \quad (2)$$

where k_l is the conductivity of the liquid, c_{pl} the specific heat of the liquid at constant pressure, ρ_l the density of the liquid, ρ_v the density of the vapor, σ the surface tension of the liquid, μ_l the viscosity of the liquid, T_w the wall temperature, T_{sat} the saturation temperature, $p_{sat}(T_w)$ the saturation pressure at the wall temperature and p_{atm} is the atmospheric pressure and corresponds to the test condition pressure (for R-113 $k_l = 0.0705$ W/(m K), $c_{pl} = 984$ J/(kg K), $\rho_l = 1507$ kg/m^3, $\rho_v = 7.46$ kg/m^3, $\sigma = 0.017$ N/m, $\mu_l = 516 \times 10^{-6}$ Pa s, $h_{lv} = 143.8$ kJ/kg and $T_{sat} = 320.75$ K).

Cooper's correlation [12] is based on the liquid reduced pressure and on the heater surface roughness, and it has been recommended by Collier and Thome [13] and Stephan [10]. It is given as,

$$h_{Cooper} = 55 p_r^b \left(-0.4343 \ln p_r\right)^{-0.55} M^{-0.5} q^{0.67}, \quad (3)$$

where $b = 0.12 - 0.08686 \ln(Rp)$, Rp is the surface roughness expressed in μm, p_r the reduced pressure, M the molecular weight, (for the R-113, $p_{cr} = 3.411 \times 10^6$ Pa, $M = 187.4$ kg/kmol). When the surface roughness is unknown, Cooper recommends Rp equal to 1 μm. We remark that the relation between the heat transfer coefficient and the heat flux in Cooper's correlation is a power equal to 2/3, as in the analysis of Ishibashi and Nishikawa [9], for an isolated bubble regime (see Eq. (1)).

In this introduction, we have focused our attention on some particular characteristics of the nucleate boiling regime. The effects of the heat flux level, the tilt angle, the surface characteristics, and the existence of two different nucleate boiling regimes have been considered. The results of this short review show that nucleate boiling with moderate heat flux exhibits a particular complexity that is not yet fully understood.

2. Experimental apparatus

A schematic drawing of the test apparatus is presented in Fig. 1 [14]. The boiling tests have been performed on the internal surface of two aluminum tubes, the internal surface of one of them being smooth, and the other grooved.

The boiler vessel is a Pyrex glass container with a stainless steel cover. It is covered by a serpentine that circulates water with the temperature controlled by a LAUDA thermal bath (see 1 in Fig. 1). The working fluid is the 113 refrigerant (R-113), at the atmospheric pressure, which corresponding saturation temperature is equal to 47.6°C. The R-113 vapor collected at the top of the boiler vessel is condensed in a water-cooled condenser (see 2 in Fig. 1) and returned to the boiler by gravity.

The smooth tube has the following dimensions: inside diameter (ID), outside diameter (OD) and length (L) equal to 16.64 ± 0.05, 18.99 ± 0.04 and 40 mm, respectively. The smooth tube is anodized and the average roughness Rp of the inside surface is 2.2 μm. The grooved tube has the following dimensions: $ID = 15.88 \pm 0.04$, $OD = 19.11 \pm 0.04$ and $L = 40$ mm. The internal surface of the grooved tube has circumferential grooves made by ERNO of Germany. The geometrical form of the grooves is shown in Fig. 2, whose main dimensions are 33 ± 7 μm of opening and 310 ± 59 μm of depth with a step of 215 μm, as is shown in Bazzo et al. [4].

The aluminum tube is monitored with five thermocouples (Tc 1–5) of type E (Chromel-Constantan), whose cable diameters are equal to 0.127 mm, attached with OMEGA cement, inside holes with 0.8 mm of diameter, and 0.2 mm of depth on the outer wall of the tubes, as shown in Fig. 3. The locations of the thermocouples on the test section are shown in Fig. 4. The

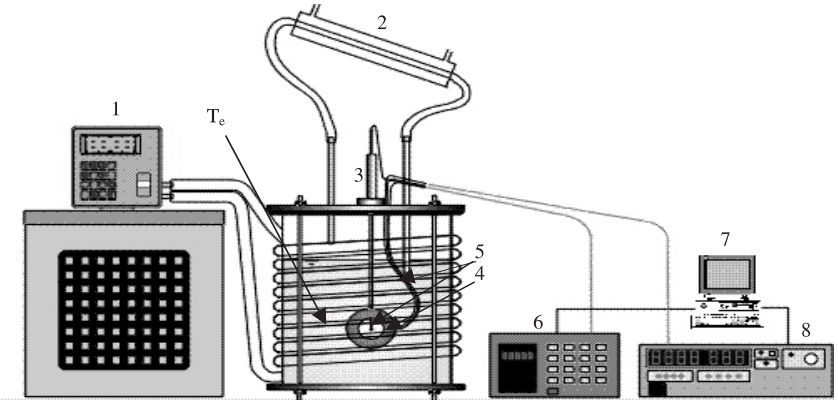

Fig. 1. Test apparatus: 1 – LAUDA thermal bath; 2 – condenser; 3 – boiler vessel; 4 – test section; 5 – thermocouples; 6 – data acquisition system; 7 – microcomputer; 8 – power supply.

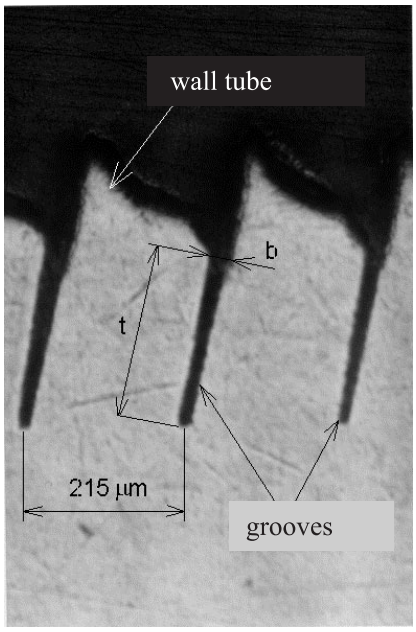

b: opening = 33±7 μm

t: depth = 310±59 μm

Fig. 2. Cross-section of the grooved tube.

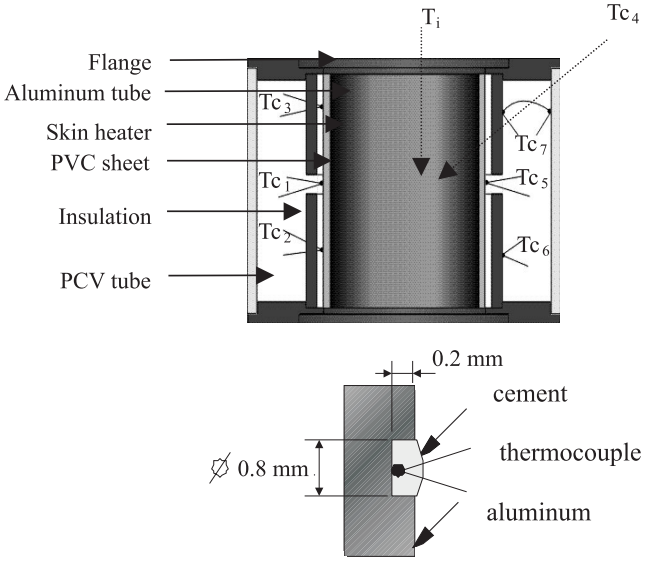

Fig. 3. Scheme of the test section.

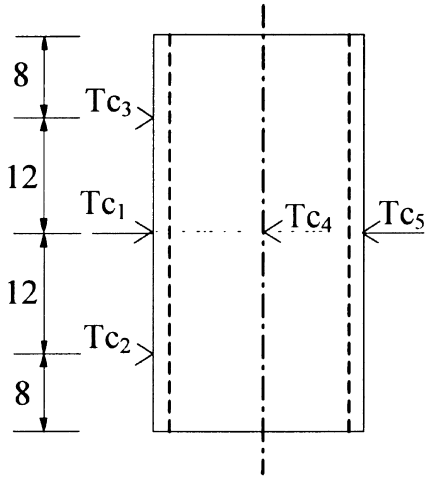

Fig. 4. Locations of the thermocouples.

heating of each aluminum tube is accomplished by two electrical skin heaters, (produced by the Laboratory of Porous Media and Thermophysical Properties (LMPT) of Federal University of Santa Catarina (UFSC)), which are attached on the outer surface of the tube and covered by a PVC tube. The electrical skin heaters are connected in parallel, and their equivalent resistances for smooth and grooved tubes are equal to 5.32 and 5.17 Ω, respectively. Finally, this set is covered by a second PVC tube and the annular space between the PVC tubes is insulated. A type E thermocouple (Tc_6) is located on the outside surface of the internal PVC tube, see Fig. 3. A differential thermocouple type K, Tc_7, in Fig. 3, allows for the measurement of the equivalent temperature difference between the outside surface of the internal PVC tube and the inner surface of the external PVC tube. By means the Tc_6 and Tc_7 signals the heating losses from the outside of the test section were estimated.

Two type E thermocouples are placed in the R-113, one of them on the axis of the tube, T_i, (at the middle of the tube length) and the second one outside of the tube.

The thermocouple signals and the voltage at the skin heater ends are recorded by a data acquisition system HP3497A (see 6 in Fig. 1) then transferred to a micro-

computer. The electrical input to the test section is delivered by means of a power supply HP6030A (0–200 V and 0–17 A) (see 8 in Fig. 1) controlled by a microcomputer (see 7 in Fig. 1).

3. Experimental procedures

The heating of the test section was controlled by a C language program, allowing a voltage step varying from zero up to a fixed value, V_1. The data was acquired after the system reached the steady state condition. In general, the quasi-steady state condition, indicated by the thermocouple signals history, was reached 90 s from the power input during the natural convection regime and 40 s during the boiling regime. After the first data acquisition, a new level voltage, V_2, was applied and new data was acquired.

Fig. 5 shows the time evolution of the wall temperature (Fig. 5a) indicated by thermocouple 2 (Tc_2), and the R-113 temperature inside a vertical grooved tube indicated by the T_i thermocouple, and the voltage signal (Fig. 5b), allowing for the characterization of the tests.

The temperature decrease of the liquid, observed in Fig. 5a, when the electrical power is delivered, indicates

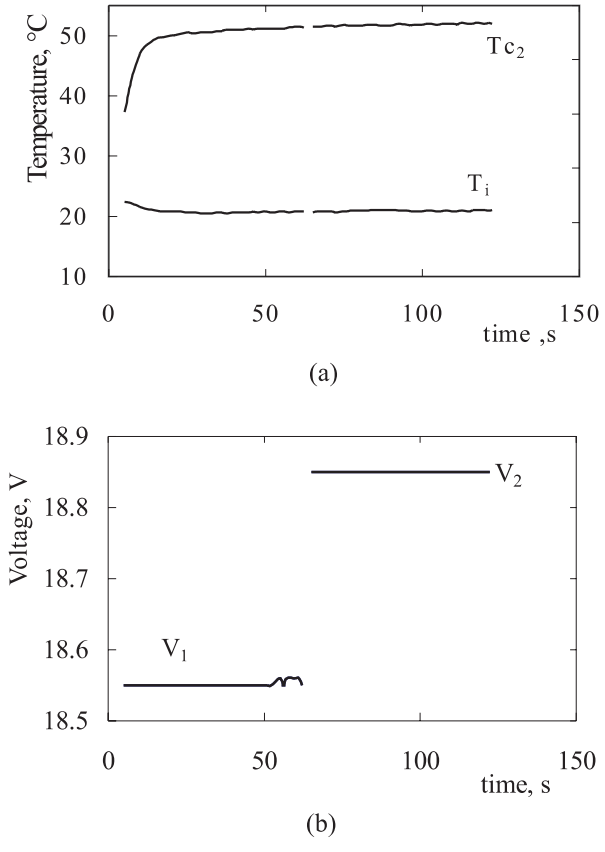

Fig. 5. Test characterizations inside a vertical grooved tube: (a) time evolution of the tube wall and liquid temperatures; (b) time evolution of the applied voltage.

a natural convection flow as an effect of the buoyancy force. The density gradients in the fluid inside the tube promote a chimney effect with the rising of the colder liquid.

3.1. Experimental uncertainty

The type E thermocouple signals were compared to the indication of the mercury-in-glass thermometers whose resolution is equal to 0.10 K, by immersion in a water bath, for the temperature range 40–90°C. Millivolts were converted to degrees by means of a ninth-order polynomial [15], and the standard deviation from the corresponding temperature indicated by the mercury-in-glass thermometer was equal to 0.3 K. The product of the t-student value ($t = 2$) for a sample of 55 degrees of freedom, with a 95% confidence level, [16], times the standard deviation, and furnishes the experimental uncertainty equal to ±0.6 K.

The experimental uncertainty of the value of the heat transfer coefficient was computed following the procedure presented by Kline [17] and Holman [15]. The relative uncertainty values for q are equal to ±3.5% and ±2% for a heat flux of 5 and 45 kW/m^2, respectively. The relative uncertainty values for the experimental heat transfer coefficient, h, are equal to ±11% and ±6%, for a heat flux of 5 and 45 kW/m^2, respectively.

3.2. Data reduction

The mean heat flux, q, delivered to the aluminum tube wall is computed in function by the net energy delivered to the R-113, Q_{net}, as well as the nominal area, A, of the inside tube surface, $q = Q_{net}/A$. The mean heat transfer coefficient, h, is computed in function by the difference between the mean wall temperature, T_w, and the saturation temperature, T_{sat}, as follows

$$h = q/(T_w - T_{sat}). \quad (4)$$

Eq. (4) is used even for sub-cooled boiling. As is considered by Carey [11, Chapter 7], the sub-cooling effect tends to disappear by increasing the heat flux.

4. Results and discussion

4.1. Nucleate boiling for vertical tubes

Fig. 6 presents the time evolution of the wall and liquid temperatures during a test with the vertical smooth tube and the corresponding heat flux delivered to R-113. The temperature decrease, near 110 s, indicates the nucleation phenomenon and can be explained by the wall contact of the colder liquid after the bubble departure. These data show that the wall superheat is equal to 14.4 K and the heat flux is 18.14 kW/m^2. The new step stabilization of the wall temperature, after 110 s, indicates a wall sperheat equal to 10.8 K. These data cannot be considered representative of the onset of nucleate boiling because this phenomenon is very much

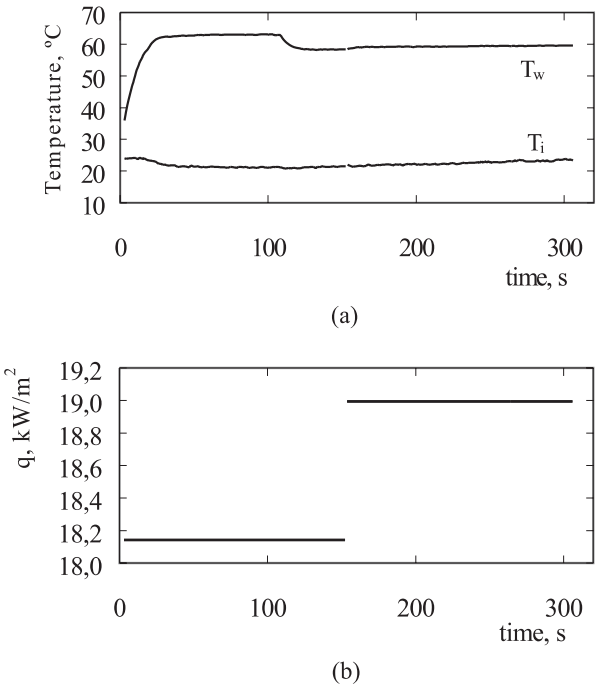

Fig. 6. Wall and fluid temperature during a test inside smooth tube: (a) time evolution of the average wall and liquid temperatures; (b) time evolution of the heat flux delivered to the R-113.

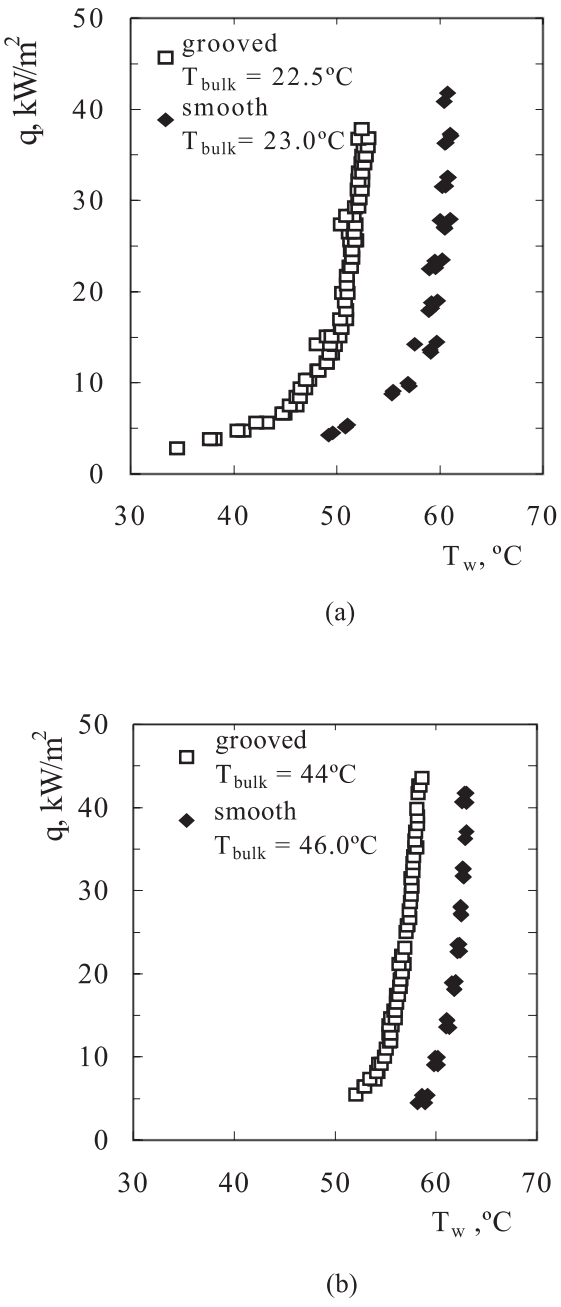

Fig. 7. Boiling curves for vertical tubes: (a) smooth; (b) grooved.

influenced by the surface characteristics (remember that the roughness of the internal surface, the average value of *Rp*, was 2.2 μm, which characterizes a smooth surface). A more detailed investigation of the nucleation phenomenon for the conditions of this work is presented in [14].

The heat flux q is plotted against the wall temperature T_w for the nucleate boiling regime for smooth and grooved vertical tubes in Fig. 7a, for bulk temperatures of 22.5°C and 23.0°C; and, in Fig. 7b, for bulk temperatures of 44.0°C and 46.0°C. For simplicity these curves have been named boiling curves. We observed that, at an identical heat flux, the wall temperatures are lower for the grooved tube. For the same tube we can observe that wall temperatures increase with the increasing bulk temperature. This trend has been observed by others as well, [7,11,18]. The lower wall temperature, for the same heat flux, shows a better heat transfer condition for the grooved tube than for the smooth tube, confirming the boiling enhancement at the low heat flux region of the nucleate regime. The experimental points of Fig. 7a are obtained for the same test conditions at different tests. We can observe a good data repeatability for the nucleate regime. However, the cooling wall effect, during the nucleation, is not so clear in this figure, in comparison with the results of the test presented in the Fig. 6a.

4.2. Nucleate boiling for horizontal tubes

The nucleate boiling curves for both smooth and grooved tubes are shown in Fig. 8. In both cases wall temperatures are lower at the top of the tube than that at the bottom; the differences are bigger in the case of the grooved tube.

For all the cases in the horizontal configuration discussed in this work, the boiling was characterized by the presence of an elongated bubble at the top and throughout the length of the tube. A schematic illustrating of the liquid–vapor configuration is shown in Fig. 9, with a representation of the cross-section in Fig. 9a and a side view of the tube in Fig. 9b which shows an elongated bubble with large bubbles escaping from the open ends and isolated bubbles on the bottom

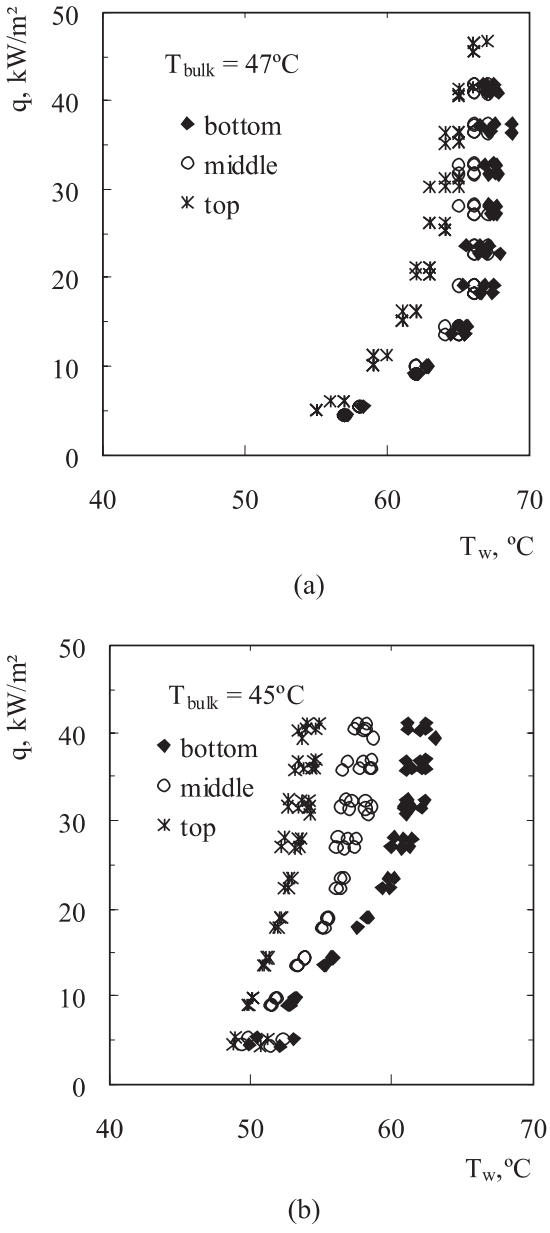

Fig. 8. Boiling curves for horizontal tubes: (a) smooth; (b) grooved.

and sides of the tube. This liquid–vapor configuration is confirmed through visualization, by means of a video camera. The wall temperature measurements show the existence of a temperature gradient in the azimuthal direction of the aluminum tube, with the lower temperature at the top region. For the smooth tube this difference is attributed to the vaporization of a liquid film between the elongated bubble and the wall, as was postulated by Ishibashi and Nishikawa [9] as well as by Nishikawa and Fujita [1]. The same mechanism can also be attributed to the temperature difference in the grooved tube, and in addition, the cooling effect of the rising liquid within the grooves.

The visualization of the internal surface in the bottom region of the smooth tube showed the presence of separated and isolated bubbles, which characterizes the non-developed nucleate boiling regime for the heat flux level of this study.

4.3. Correlation analysis

The comparison between the experimental heat transfer coefficient and the corresponding values correlated by the Forster–Zuber and the Cooper correlations, with $Rp = 33$ μm, is presented in Fig. 10. The comparison between the values computed by both correlations show that the roughness effect, for $Rp = 33$ μm, is superestimated by the Cooper's correlation as we can observe in Fig. 10a–c. We can observe that (see Fig. 10a–c) for the grooved tube, the experimental values are higher than those computed by Forster–Zuber correlation. When the sub-cooling of the liquid is high, for $T_{bulk} = 22.5$°C (T_{sat} for R-113, at normal atmospheric pressure, is equal to 47.6°C), the experimental values are higher than the correlated values, with a mean deviation of 91.5%, see Table 1. For a condition of $T_{bulk} = 44.0$°C, very close to the saturation, the experimental values are also higher than the correlated values with a mean deviation of 45.6% and the difference increases for high heat flux, as shown in Fig. 10b. A similar behavior is observed for a horizontal tube (see Fig. 10c) for a condition very close to the saturation, whose mean deviation is 56.8%. For the smooth tube, the comparisons between the experimental values and those computed by

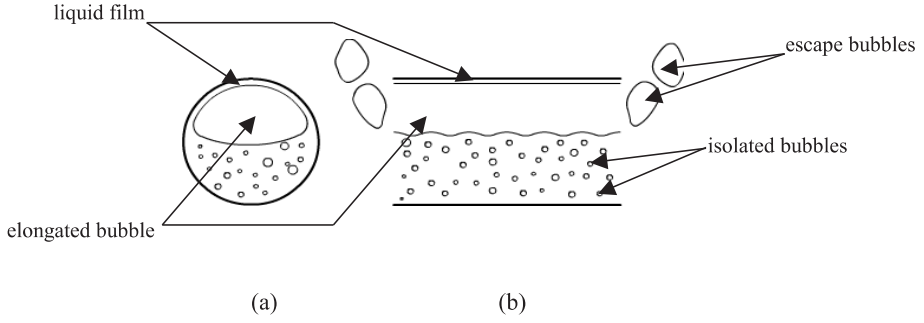

Fig. 9. Schematic illustrating the two-phase configuration during boiling tests in horizontal tubes: (a) cross-section; (b) side view.

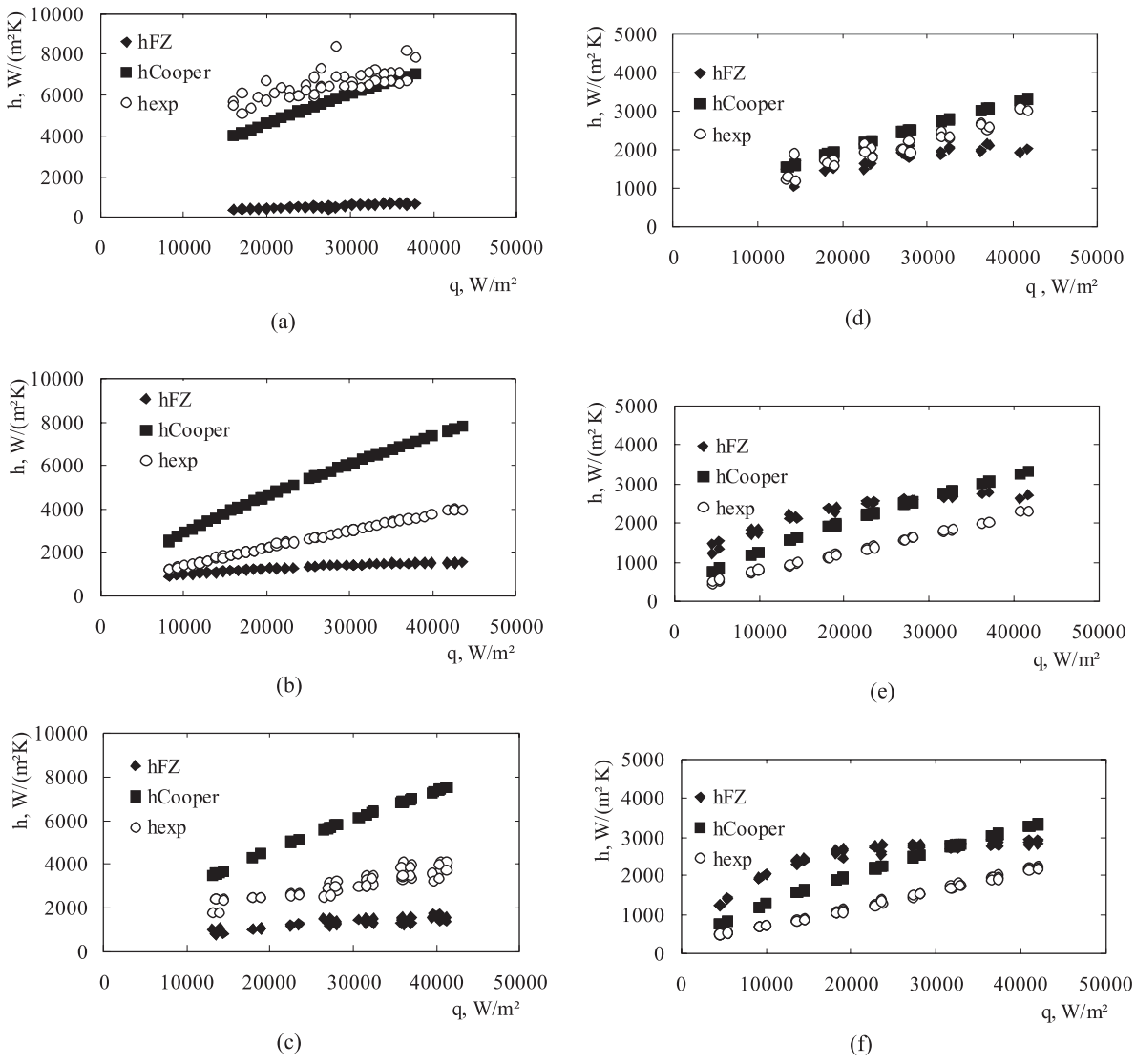

Fig. 10. Experimental and correlated heat transfer coefficient: (a) vertical grooved tube, $T_{bulk} = 22.5°C$; (b) vertical grooved tube, $T_{bulk} = 44.0°C$; (c) horizontal grooved tube, $T_{bulk} = 45.0°C$; (d) vertical smooth tube, $T_{bulk} = 23.0°C$; (e) vertical smooth tube, $T_{bulk} = 46.0°C$; (f) horizontal smooth tube, $T_{bulk} = 47.0°C$.

Table 1
Statistical comparison of the correlations[a]

Tube configuration	Internal surface	T_i (°C)	Mean deviation[b] (%) Cooper	Mean deviation (%) Forster–Zuber
V	G	22.5	14.14	91.5
V	G	44.0	104.48	45.6
H	G	45.0	91.20	56.8
V	S	23.0	16.7	19.3
V	S	46.0	59.2	96.2
H	S	47.0	66.2	109.4

[a] G: grooved; S: smooth; V: vertical; H: horizontal.
[b] Mean deviation $= 1/N \sum(|h_{exp} - h_{correlation}|/h_{exp}) \times 100\%$.

the Forster–Zuber and the Cooper correlations, with $Rp = 2.2$ μm, are presented in Fig. 10d–f. For all the cases, the Cooper correlation gives values higher than those of the present data. However, opposite to the expected trend, the differences between the Cooper correlated values and the experimental data increase when T_{bulk} get closed to T_{sat}. The comparison with Cooper correlation shows that the mean deviation between the

experimental values and those predicted is equal to 16.7%, 59.2% and 66.2% as shown in Fig. 10d–f, respectively, and in Table 1. For the Forster–Zuber correlation the mean deviation is equal to 19.3%, 96.2%, and 109.4% as shown in Fig. 10d–f, respectively, and in Table 1. For bulk temperature close to the saturation temperature the difference decreases when the heat flux increases, as is expected because Forster–Zuber correlation is valid for developed saturated boiling.

An analysis of the experimental data, for the grooved tube with T_{bulk} equal to 44°C, and also for the smooth tube with T_{bulk} equal to 46°C, showed that h is related to q by means of a power near to 2/3. Considering only the data for the smooth tube the average value of n is equal to 0.75 [14]. These results agree with the literature about the nucleate boiling regime [9,10].

5. Practical significance

The experimental data presented in this work show the increase of the heat transfer coefficient for internal enhanced surface of a tube consisted of microgrooves. These results have practical significance, as in the case for capillary pumps and two-phase solar thermosyphons applications. The results for horizontal tube can be useful for the thermal analysis of evaporators of refrigerant cycles.

6. Conclusions

We have presented new experimental results on nucleate pool boiling inside vertical and horizontal aluminum open-ended tubes whose internal surfaces are either smooth or grooved. The tests were performed at the LABSOLAR/NCTS in the Department of Mechanical Engineering at the Federal University of Santa Catarina.

The main results in this work are the following:

(i) At moderate heat flux ($q < 40$ kW/m^2) boiling heat transfer depends on the liquid bulk temperature; and the wall temperature decreases as an effect of the bulk temperature decrease;

(ii) For all the tests, the heat transfer coefficient of the grooved tube is higher than that of the smooth tube;

(iii) For a smooth vertical tube, the relation between h and q^n occurs for an average value of n equal to 0.75;

(iv) The experimental values of the heat transfer coefficient for a vertical smooth tube show the trend for data to agree with those values computed by the Forster–Zuber correlation;

(v) Tests inside horizontal tubes present a temperature gradient in the azimuthal direction, with a lower temperature at the top. This behavior results of two different boiling mechanisms related to the presence of an elongated bubble throughout the tube length, at the top region, and the isolated bubbles on the bottom of the tube. This temperature difference is higher for a grooved tube than for a smooth tube.

Acknowledgements

The authors wish to express their gratitude to Dr. Saulo Güths who furnished the skin-heater. One of the authors, RFR, thanks CAPES for providing a scholarship. This research was supported by *CNPq* (523068/94-8) and *AEB* (Brazilian Space Agency).

References

[1] K. Nishikawa, Y. Fujita, Nucleate boiling heat transfer and its augmentation, in: J.P. Hartnett, T.F. Irvine Jr. (Eds.), Advances in Heat Transfer, vol. 20, Academic Press, New York, 1990, pp. 1–82.

[2] P.J. Marto, L.V.J. Lepere, Pool boiling heat transfer from enhanced surfaces to dielectric fluids, Transactions of the ASME-Journal of Heat Transfer 104 (1982) 292–299.

[3] T. Fujii, S. Koyama, N. Inoue, K. Kuwahara, S. Hirakuni, An experimental study of evaporation heat transfer of refrigerant HCFC22 inside an internally grooved horizontal tube, JSME International Journal B38 (4) (1995) 618–627.

[4] E. Bazzo, J.C. Passos, S. Colle, Comportamento Térmico de Bombas Capilares de Ranhuras Circunferenciais, in: Sixth Brazilian Congress of Engineering and Thermal Sciences and Sixth Latin American Congress of Heat and Mass Transfer, Florianópolis, Brazil, vol. II, November 1996, pp. 889–893.

[5] J.C. Passos, Design of a Confined Boiling Experiment under Microgravity to Fly in theMicro Satellite/France-Brazil, INPE/ABC, Approved Design by the Academia Brasileira de Ciências-RJ, February 1997.

[6] A.E. Bergles, Some perspectives on enhanced heat transfer-second generation heat transfer technology, Transactions of the ASME-Journal of Heat Transfer 110 (1988) 1082–1087.

[7] J.R. Thome, Enhanced Boiling Heat Transfer, Hemisphere, Washington, DC, 1990.

[8] R.L. Webb, Principles of Enhanced Heat Transfer, Wiley, New York, 1994.

[9] E. Ishibashi, K. Nishikawa, Saturated boiling heat transfer in narrow spaces, International Journal of Heat and Mass Transfer 12 (1969) 863–894.

[10] K. Stephan, Heat Transfer in Condensation and Boiling, Springer, Berlin, 1992.

[11] V.P. Carey, Liquid–Vapor Phase-Change Phenomena, Hemisphere, Washington, DC, 1992.

[12] M.G. Cooper, Saturation nucleate pool boiling- a simple correlation, International Chemical Engineering Symposium Series 86 (1984) 785–792.

[13] J.G. Collier, J.R. Thome, Convective Boiling and Condensation, third ed., Oxford University Press, Oxford, 1994.

[14] R.F. Reinaldo, Experimental study of the nucleate boiling on grooved and smooth cylindrical surfaces, M.Sc. Dissertation, Graduate Program on Mechanical Engineering, Federal University of Santa Catarina, Brazil, 1999 (in Portuguese).

[15] J.P. Holman, Experimental Methods for Engineers, McGraw-Hill, New York, 1989.

[16] ASME, Measurement Uncertainty, ANSI/ASME Power Test Code 19-1-1985/ASME, New York, 1986.
[17] S.J. Kline, The purposes of uncertainty analysis, ASME Journal of Fluid Engineering 107 (1985) 153–160.
[18] R.F. Reinaldo, S. Güths, J.C. Passos, Nucleate boiling on grooved and smooth tube surfaces, in: Seventh Brazilian Congress of Engineering and Thermal Sciences, Rio de Janeiro, Brazil, vol. I, November 1998, pp. 649–653.